CLUSTER FEATURES IN REACTIONS AND STRUCTURE OF HEAVY NUCLEI

G.G. Adamian[a,b,c], N.V. Antonenko[a,c], R.V. Jolos[a,c], W. Scheid[c] and T.M. Shneidman[c]

[a]Joint Institute for Nuclear Research, 141980 Dubna, Russia
[b]Institute of Nuclear Physics, Tashkent 702132, Uzbekistan
[c]Institut für Theoretische Physik der Justus-Liebig-Universität
35392 Giessen, Germany

(Received September 23, 2002)

Dedicated to Adam Sobiczewski in honour of his 70th birthday

Cluster effects in the structure of heavy nuclei are considered. The properties of the states of the alternating parity bands in Ra, Th, U and Pu isotopes are analyzed within a cluster model. The model is based on the assumption that cluster type shapes are produced by the motion of the nuclear system in the mass asymmetry coordinate. The results of calculations of the spin dependence of the parity splitting and of the electric multipole transition moments are in agreement with the experimental data.

PACS numbers: 21.60.Ev, 21.60.Gx

1. Introduction

Cluster states are intensively investigated in the light nuclei [1]. They are discussed also in connection with the properties of heavy nuclei [2–5] where they are manifested in nuclear structure and reactions. However, cluster states are better seen in the strongly deformed configurations which can be formed in heavy ion fusion reactions used to populate high-spin deformed and superdeformed states.

Cluster states in fusion of heavy nuclei: The fusion of two heavy nuclei is a multidimensional process. The choice of the most important collective variables needed for its description is a complicated problem. It is a common opinion that the most important degrees of freedom are the elongation of the total system, mirror asymmetry and neck radius [6]. Depending on a trajectory in this three dimensional configurational space, two approaches to the description of nuclear fusion can be imagined. One of them is based on the picture of the neck formation between interacting nuclei and a subsequent increase of a neck radius up to the value corresponding to a deformed compound nucleus. The other one is related to the mass asymmetry increase in a system of two interacting nuclei, when nucleons are transfered from the light to the heavy cluster up to formation of a mononucleus [7, 8]. This approach allows us to describe a lot of experimental data on fusion of heavy nuclei, especially the production of superheavy ones.

Any model of the collective motion (fusion is of course a collective motion) is described by a Hamiltonian consisting of the two parts: the kinetic energy and the potential energy terms. If the selected collective variables are strongly coupled to the intrinsic degrees of freedom, which are not explicitly presented in the Hamiltonian, a dissipative term (nuclear friction) should be included into consideration and a process should be treated in the framework of the kinetic approach. The potential energy as a function of the collective variables has been investigated in many publications and is rather well understood. The inertia coefficients are rather less investigated [9–12]. However, inertia tensor is a very important ingredient of any collective model. In fact, the inertia tensor is related to the nondiagonal matrix elements of the Hamiltonian taken between configurations which are characterized by different localization in the configurational space, and strongly influences on the type of the trajectory along which the system evolves in the configurational space. Set of the diagonal matrix elements of the Hamiltonian is the potential energy. Smaller nondiagonal matrix elements correspond to larger inertia coefficients and *vice versa*. In the case of dissipation and an application of the kinetic approach transitions between two configurations are described by diffusion coefficients. Again the larger diffusion coefficient in coordinate corresponds to smaller inertia and *vice versa*. It is clear from the Inglis formula that inertia depends strongly on a density of the single particle states near the Fermi surface. Investigating a dependence of the component of the inertia tensor related to the neck degree of freedom, it was shown in [13] that this inertia parameter is much larger than one obtained within the hydrodynamical model and as a consequence the growth of neck between interacting nuclei less probable. This large value of the inertia stabilizes a value of the neck radius during a reaction. In addition, the structural forbiddenness effect (Pauli principle) hinders the motion to smaller internuclear distances [14, 15] Due to these reasons dinuclear type configuration, which is in fact a cluster type configuration, survives for a sufficiently long time and evolves along the mass asymmetry degree of freedom, transforming from a one cluster configuration to the other with different mass partition between clusters. This stabilization of a relatively small neck radius during a fusion process regards the interplay between order and chaos in a nuclear system. When a neck radius is small the nearest neighbor level spacing distribution of a single particle spectra is described by Poisson distribution [16]. However, it approaches the Wigner distribution if a neck radius increases. Thus, configuration with a small neck radius corresponds to a regular single particle motion, *i.e.* to a motion stable against chaos. With a neck radius increase (before approaching the following stable configuration) a single particle motion becomes unstable against chaos. Thus, we see that the effects of clusterization can be seen in the fusion reactions leading to a formation of heavy nuclei.

Cluster states in deformed light and heavy nuclei: Different stable deformed configurations of light and heavy nuclei can be investigated using the Nilsson–Strutinsky or the Hartree–Fock methods. The spectroscopic properties of octupole-deformed, superdeformed and reflection-asymmetric hyperdeformed minima of multidimensional potential surface have been discussed in [3, 4, 17–19] Different stable deformed configurations of nuclei can be investigated using the Nilsson–Strutinsky or the Hartree–Fock methods. The calculations for light nuclei and actinides [3, 4, 20, 21] have shown that configurations with large equilibrium deformations are strongly related to the clustering. Recent theoretical emphases has been done on the relation of the clustering to the symmetries of a deformed single particle nuclear potential. As is well known, when the harmonic oscillator becomes deformed the degeneracy of the single particle states, which is presented at zero deformation, is lost at first, however, recreated again when a ratio of the frequencies of the harmonic oscillator $\omega_\perp : \omega_z$ becomes equal to the ratio of the integer numbers $n : 1$ with $n = 2, 3, 4, \ldots$ The clustering may be an important structural feature at these deformations because the magic numbers associated with the corresponding shell gaps are expressed as combinations of the spherical magic numbers [21]. This feature was stressed in the application of the group theory to deformed harmonic oscillator [2]. At the integer ratios of the axial symmetry deformations $\omega_\perp : \omega_z = n : 1$ the symmetry of the many particle wave function can be classified in terms of the irreducible representations of n SU(3) groups coupled together. This feature admits a description of the deformed harmonic oscillator in terms of a series of overlapping spherical potentials [21]. In this description a deformation process can be viewed as a division of the original spherical potential into a series of smaller potentials aligned along the deformation axis [21]. Fusion can be considered in this picture as a process of the mass exchange between the potentials in agreement with the discussion presented above.

The well known example of the molecular-like structures in light nuclei are the ground state bands of ^{8}Be, ^{20}Ne and the excited band in ^{16}O based on the 0^+ (6.06 MeV) state. The rotational bands in ^{8}Be and ^{20}Ne have large moments of inertia expected for the systems of two clusters in a contact:

^{4}He + ^{4}He in the case of ^{8}Be and ^{16}O + ^{4}He in the case of ^{20}Ne. The large α-decay widths of these rotational levels indicate that these band states have bimolecular structure.

A direct and very important consequence of the asymmetric cluster-type structures like ^{12}C + ^{4}He (^{16}O*) and ^{16}O + ^{4}He (^{20}Ne) is a presence of the negative parity rotational states with odd angular momenta together with the positive parity rotational states having even angular momenta. The negative parity states are shifted up with respect to the positive parity ones since there is a non negligible penetration probability of the barrier separating the configurations with α-cluster located to the left and to the right from the heavier cluster. Indeed, such negative parity rotational states are observed in ^{16}O* and ^{20}Ne. The positive and negative parity states taken together form alternating parity band. It is very interesting that such bands are known not only in light, but also in the heavy nuclei: in isotopes of Rn, Ra, Th, U, and Pu. They are considered frequently as related to the octupole deformation. However, using the ideas discussed above that a deformation can be treated as a motion (exchange) of a mass between the clusters, we can apply the model based on the Hamiltonian with the mass asymmetry degree of freedom as the main collective variable to the description of the alternating parity bands in heavy nuclei.

2. Cluster model of fusion of heavy nuclei

Nuclear systems consisting of a heavy cluster A_1 plus a light cluster A_2 belong to the class of dinuclear-type shapes. They were introduced to explain data on deep inelastic and fusion reactions with heavy ions [22]. The dinuclear system model of fusion [7, 8] considers the fusion as a diffusion of the dinuclear system in the mass asymmetry, defined by

$$\eta = \frac{A_1 - A_2}{A_1 + A_2}$$

(A_1 and A_2 are the mass numbers of the nuclei of dinuclear system). The potential barrier in η supplies a hindrance for fusion. In the dinuclear system model the evaporation residue cross section is factorized as

$$\sigma_{\mathrm{ER}}(E_{\mathrm{c.m.}}) = \sum_J \sigma_c(E_{\mathrm{c.m.}}, J) P_{\mathrm{CN}}(E_{\mathrm{c.m.}}, J) W_{\mathrm{sur}}(E_{\mathrm{c.m.}}, J)\,. \tag{1}$$

Here, σ_c is the partial capture cross section for the transition of the colliding nuclei over the Coulomb barrier. The contributing angular momenta are limited by the survival probability $W_{\mathrm{sur}}(E_{\mathrm{c.m.}}, J)$. The probability of complete fusion P_{CN}, dependent on nuclear structure effects and on the neutron excess above the nearest closed shells in the colliding nuclei, is very important for the correct calculation of $\sigma_{\rm ER}$. $P_{\rm CN}$ describes the competition between complete fusion and quasifission (decay of the dinuclear system after the capture stage).

The experimental evaporation residue cross sections [23, 24] in cold (^{208}Pb- and ^{209}Bi-based) and hot (actinide-based) fusion reactions leading to the production of heavy and superheavy nuclei (Z = 104–116) are well reproduced (Fig. 1).

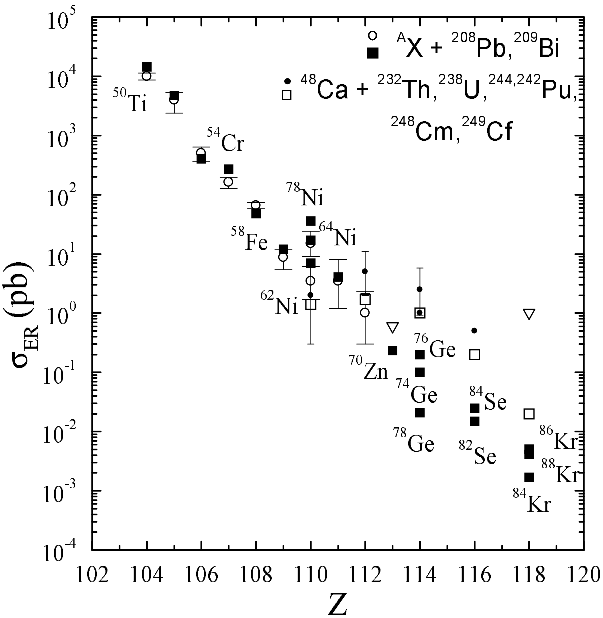

Fig. 1. Evaporation residue cross sections for cold and hot fusion reactions as a function of the charge number of the superheavy nucleus. The calculated data are shown by the squares. The open triangles give experimental upper limits.

3. Dinuclear model in nuclear structure

3.1. Mass asymmetry coordinate in description of nuclear shape

Instead of parameterization of the nuclear shape in terms of quadrupole, octupole and higher multipole deformations, the mass asymmetry coordinate η and the distance R between the centers of clusters are used as relevant collective variables [1]. The ground state wave function in η can be thought as a superposition of different cluster-type configurations including the mononucleus configuration with $|\eta|$=1. The relative contribution of each cluster component to the total wave function is determined by the collective

Hamiltonian

$$H = -\frac{\hbar^2}{2B_\eta}\frac{d^2}{d\eta^2} + U(\eta, I)\,, \qquad (2)$$

where B_η is the effective mass and $U(\eta, I)$ is the potential. In order to calculate the dependence of the parity splitting on the angular momentum, we search for solutions of the stationary Schrödinger equation describing the dynamics in η:

$$H\,\Psi_n(\eta, I) = E_n(I)\,\Psi_n(\eta, I)\,. \qquad (3)$$

The eigenfunctions Ψ_n of this Hamiltonian have a well defined parity with respect to the reflection $\eta \to -\eta$ which corresponds to the space reflection. The potential $U(\eta, I)$ in Eq. (2) is taken for $|\eta| < 1$ as a dinuclear potential energy

$$U(\eta, I) = B_1(\eta) + B_2(\eta) - B + V(R = R_m(\eta), \eta, I)\,. \qquad (4)$$

Here, the internuclear distance $R_m(\eta)$ is the touching distance between the clusters and is set to be equal to the value corresponding to the minimum of the potential in R for a given η. The quantities B_1 and B_2 (which are negative) are the experimental binding energies of the clusters forming the dinuclear system at a given η, and B is the binding energy of the mononucleus. The nucleus-nucleus interaction potential in (4) is given as

$$V(R, \eta, I) = V_{\rm coul}(R, \eta) + V_N(R, \eta) + V_{\rm rot}(R, \eta, I) \qquad (5)$$

with the Coulomb $V_{\rm coul}$, the centrifugal $V_{\rm rot}$ and the nuclear interaction V_N potentials. The potential V_N is obtained with a double folding procedure using the ground state nuclear densities of the clusters. Antisymmetrization between the nucleons belonging to different clusters is regarded by a density dependence of the nucleon–nucleon force which gives a repulsive core in the cluster–cluster interaction potential. Details of the calculation of V_N are given in [25]. The nucleus–nucleus potential $V(R, \eta, I)$ and potential U ("driving potential") were successfully applied to the analysis of the experimental data on fusion and deep inelastic reactions with heavy ions [25, 26].

Our calculations have shown that in the cases of Ra, Th, U and Pu isotopes the dinuclear configuration with an alpha cluster has a potential energy which is close or even smaller than the energy of the mononucleus at $|\eta| = 1$ [27]. The energies of the Li-cluster configurations are about 15 MeV larger than the binding energies of the mononuclei considered. Therefore, for small excitations only oscillations in η are of interest which lie in the vicinity of $|\eta|=1$.

To calculate the potential energy for $I \neq 0$, the moment of inertia $\Im(\eta) = \Im(\eta, R_m)$ in the rotational energy term in Eq. (5) has to be fixed. It is known that the moments of inertia of superdeformed states are about 85% of the rigid-body limit [28]. As was shown in [29], the equilibrium deformations and the moments of inertia of the highly deformed states are well described if we consider them as cluster systems. Therefore, we assume that the moment of inertia of the cluster configurations can be expressed as

$$\Im(\eta) = c_1 \left(\Im_1^{\mathrm{r}} + \Im_2^{\mathrm{r}} + m_0 \frac{A_1 A_2}{A} R_m^2 \right) . \tag{6}$$

Here, $\Im_i^{\mathrm{r}}, (i = 1,2)$ are the rigid body moments of inertia for the clusters, c_1=0.85 [28] for all considered nuclei and m_0 is the nucleon mass. For $|\eta| = 1$, the value of the moment of inertia is not known from the data because the experimental moment of inertia is a mean value between the moment of inertia of the mononucleus ($|\eta|$=1) and the ones of the cluster configurations arising due to the oscillations in η. We assume that $\Im(|\eta| = 1) = c_2 \Im^{\mathrm{r}}(|\eta| = 1)$, where $\Im^{\mathrm{r}}$ is the rigid body moment of inertia of the mononucleus with A nucleons calculated with deformation parameters [30] and c_2 is a scaling parameter which is fixed by the energy of the first 2^+ state or other even parity state. The chosen values of c_2 vary in the interval $0.1 < c_2 < 0.3$.

The method of calculation of the inertia coefficient B_η is given in [31]. Although this method is more suitable for calculations of the inertia in the systems with more heavier clusters than α, the results obtained in this way can be extrapolated to the values of η close to $|\eta| = 1$. The formula obtained in [31] shows that B_η is a smooth function of the mass number A. As a consequence, we take nearly the same value of B_η=$20{\times}10^4 m_0$ fm^2 for almost all considered actinide nuclei with a variation of 10%. Only for ^{222}Th and ^{220,222}Ra we varied B_η in the range B_η=(10–20)$\times 10^4 m_0$ fm^2 to obtain the correct value of the ground state energy.

The value of B_η can be estimated also in the other way. Rewriting the Schrödinger equation (3) with the Hamiltonian (2) in a discrete form

$$\begin{aligned} &- \frac{\hbar^2}{2B_\eta(\Delta\eta)^2} \left(\psi_n(\eta + \Delta\eta) + \psi_n(\eta - \Delta\eta) - 2\psi_n(\eta)\right) + V(\eta)\psi_n(\eta) \\ &= E_n \psi_n(\eta) \end{aligned} \tag{7}$$

we obtain the following expression for the nondiagonal matrix element of the Hamiltonian in a discrete basis

$$\langle \eta + \Delta\eta | H | \eta \rangle = - \frac{\hbar^2}{2B_\eta(\Delta\eta)^2} . \tag{8}$$

For the transfer of a pair of nucleons $\Delta\eta = 4/A$. We estimate the nondiagonal matrix element of the Hamiltonian by the pairing interaction constant $G = 25/A$ MeV responsible for transfer of pairs of nucleons into the valent shells. Then $B_\eta = \hbar^2 A^3/800$. Taking $A = 230$ we obtain the value $B_\eta = 64 \times 10^4\ m_0\ \mathrm{fm}^2$, which is close to the value given above.

3.2. Description of the alternating parity bands

With Eq. (3) we first calculated the parity splitting for several isotopes of Ra, Th, U and Pu for different values of the angular momentum I. The results of calculations agree well with the experimental data [32]. The largest deviations of the calculated values from the experimental data are found in the lightest Ra and Th isotopes. As an example, the results of calculations for Th isotopes are shown in Table I. A good description of the experimental data, especially of the variation of the parity splitting with A at low I and of the value of the critical angular momentum at which the parity splitting disappears, means that the dependence of the potential energy on η and I for the considered nuclei is correctly described by our cluster model.

TABLE I

Comparison of experimental ($E_{\rm exp}$) and calculated ($E_{\rm calc}$) energies of states of the alternating parity bands in $^{232-222}$Th. Energies are given in keV. Experimental data are taken from [32, 37].

	^{232}Th		^{230}Th		^{228}Th		^{226}Th		^{224}Th		^{222}Th	
I^π	$E_{\rm exp}$	$E_{\rm calc}$	$E_{\rm exp}$	$E_{\rm calc}$	$E_{\rm exp}$	$E_{\rm calc}$	$E_{\rm exp}$	$E_{\rm calc}$	$E_{\rm exp}$	$E_{\rm calc}$	$E_{\rm exp}$	$E_{\rm calc}$
1^-	714	693	508	485	328	350	230	254	251	204	250	195
2^+	49	49	53	53	58	58	72	72	98	98	183	183
3^-	774	761	572	557	396	423	308	340	305	311	467	366
4^+	162	160	174	172	187	177	226	238	284	296	440	461
5^-	884	882	687	684	519	549	451	490	465	494	651	616
6^+	333	330	357	354	378	391	447	475	535	563	750	760
7^-	1043	1051	852	859	695	748	658	698	700	739	924	920
8^+	557	553	594	589	623	634	722	761	834	868	1094	1077
9^-	1249	1263	1065	1075	921	971	923	958	998	1036	1255	1258
10^+	827	822	880	869	912	919	1040	1079	1174	1202	1461	1430
11^-	1499	1511	1322	1326	1190	1229	1238	1263	1347	1384	1623	1624
12^+	1137	1130	1208	1215	1239	1235	1395	1424	1550	1564	1851	1815
13^-	1785	1792	1615	1629	1497	1517	1596	1609	1739	1772	2016	2019
14^+	1482	1470	1573	1565	1605	1572	1781	1796	1959	1966	2260	2226
15^-	2101	2099	1946	1941	1838	1823	1989	2002	2165	2194	2432	2450
16^+	1858	1841	1971	1935	1993	1918	2196	2200	2398	2405	2688	2663
17^-	2445	2449	2310	2274	2209	2154	2413	2429	2620	2651	2873	2906
18^+	2262	2229	2398	2318	2406	2281	2635	2640	2864	2880	3134	3128
19^-	2813	2794	2703	2624			2861	2890			3341	3380
20^+	2691	2633	2850	2709			3097	3115			3596	3621

The ground state energy level lies near the top of the barrier and the weight of the α-cluster configuration estimated as that contribution to the norm of the wave function which is located at $|\eta| \leq \eta_\alpha$ is about 5×10^{-2} for ^{226}Ra, which is close to the calculated spectroscopic factor [33]. This means that our model is in qualitative agreement with the known α-decay widths of the nuclei considered.

The spectra of those considered nuclei whose potential energy has a minimum at the alpha cluster configuration can be well approximated by the following expression

$$\begin{aligned} E(I) &= \frac{\hbar^2}{2J(I)} I[I+1], \text{ if } I \text{ is even}, \\ E(I) &= \frac{\hbar^2}{2J(I)} I[I+1] + \delta E(I), \text{ if } I \text{ is odd}, \end{aligned} \tag{9}$$

where the parity splitting $\delta E(I)$ is given as

$$\delta E(I) = \frac{2E_1(I^\pi = 1^-)}{1 + \exp(b_0 \sqrt{B_0 I[I+1]})} \tag{10}$$

with

$$B_0 = \frac{\hbar^2}{2} \left(\frac{1}{\Im(\eta = 1)} - \frac{1}{\Im(\eta = \eta_\alpha)} \right)$$

which describes the change of the height of the barrier with spin I. The moment of inertia in Eq. (9) is given by the expression

$$J(I) = w_m(I) \Im(\eta = 1) + [1 - w_m(I)] \Im(\eta = \eta_\alpha) \tag{11}$$

which contains a probability

$$w_m(I) = \frac{w_m(I = 0)}{1 + b_1 B_0 I[I+1]}, \tag{12}$$

to find the mononucleus component in the wave function of the state with spin I of the ground state band. Since $w_m(I)$ decreases with angular momentum increase, $J(I)$ increases with I. The quantity $w_\alpha(I) = 1 - w_m(I)$ gives the corresponding probability of the α-cluster component. The constants $\Im(\eta = 1) = 0.3 \Im^{\mathrm{r}}(\eta = 1)$, $w_m(I = 0)$=0.93, $b_0 = \pi$ MeV$^{-1/2}$ and $b_1 = 0.2$ MeV^{-1} were obtained by fitting the experimental data. With these constants the spectra of many nuclei are described quite well. Therefore, Eqs (9) and (10) can be used to predict the energies of the unknown levels.

3.3. Electric multipole transition moments

With the wave functions obtained, we have calculated the reduced matrix elements of the electric multipole moments $Q(\mathrm{E1})$, $Q(\mathrm{E2})$ and $Q(\mathrm{E3})$. The effective charge for E1-transitions has been taken to be equal to $e_1^{\mathrm{eff}} = e(1+\chi)$ with an average state-independent value of the $E1$ polarizability coefficient $\chi = -0.7$ [34, 35]. This renormalization takes into account a coupling of the mass-asymmetry mode to the giant dipole resonance in a dinuclear system. In the case of the quadrupole transitions we did not renormalized the charge $e_2^{\mathrm{eff}} = e$. For octupole transitions we took $e_3^{\mathrm{eff}} = e(1-0.2\tau_z)$ assuming that an additional contribution to the effective charge arises from the coupling of the mass-asymmetry mode to the higher-lying isovector and isoscalar octupole excitations [34]. The results of these calculations are listed in Table II. In general, the obtained values are in agreement with the experimental data for Q_λ^{exp} [36–39], however, with some exceptions. For instance, a small value of $D_{10}(0^+ \to 1^-)$ in ^{224}Ra is not reproduced. The higher moments are in agreement with the calculations of Ref. [30]. The calculations qualitatively reproduce the angular momentum dependence of the experimental matrix elements of the electric dipole operator.

TABLE II

Calculated and experimental intrinsic multipole transition moments. The values of the dipole moment D_{10} are given for those values of the nuclear spin I for which there are experimental data. These values of I are shown in the second column. The experimental data are taken from [32, 36–39].

Nucleus	D_{10}		$Q_{20}(0^+ \to 2^+)$		$Q_{30}(0^+ \to 3^-)$	
	(e fm) calc.	(e fm) exp.	(e fm^2) calc.	(e fm^2) exp.	(e fm^3) calc.	(e fm^3) exp.
^{220}Ra	0.28 (I=7)	0.27	397	558	3305	
^{222}Ra	0.30 (I=7)	0.27	395	675	3197	
^{224}Ra	0.133 (I=3)	0.028	510	633	2543	
^{226}Ra	0.111 (I=1)	0.06–0.10	574	718	2800	2861
^{222}Th	0.29 (I=6)	0.38	397	548	3120	
^{224}Th	0.312 (I=10)	0.52	495		2564	
^{226}Th	0.223 (I=8)	0.30	561	830	2334	
^{228}Th	0.151 (I=8)	0.12	653	843	2070	
^{230}Th	0.054 (I=6)	0.04	666	899	1720	2144
^{232}Th	0.007 (I=1)		719	966	1369	1969
^{234}U	0.004 (I=1)		758	1035	1407	1895
^{236}U	0.004 (I=1)		786	1080	1318	1951
^{238}U	0.004 (I=1)		818	1102	1313	2041

Fig. 2 illustrates the angular momentum dependence of the calculated intrinsic transition quadrupole moment. It is interesting that the cluster model shows an increase of the quadrupole moment with angular momentum in the transitional nucleus ^{226}Ra and its constancy in the well deformed ^{238}U. Staggering seen in Fig. 2 for both ^{226}Ra and ^{238}U isotopes is explained by the higher weight of the α-cluster component in the wave functions of odd I states. This cluster configuration has a larger deformation.

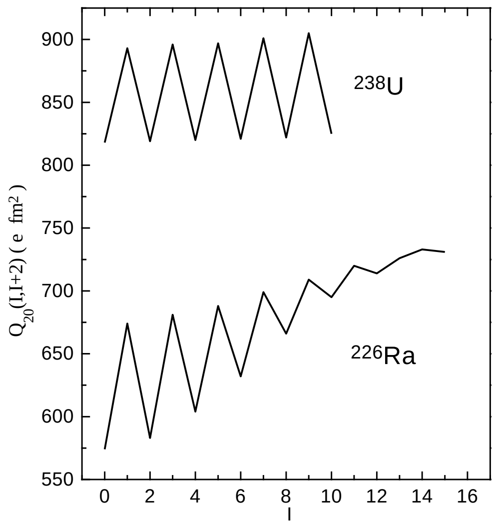

Fig. 2. Angular momentum dependence of the calculated intrinsic quadrupole transition moments in ^{226}Ra and ^{238}U.

4. Summary

In conclusion, the manifestations of the cluster effects in the reactions and structure of heavy nuclei are illustrated. A cluster interpretation of the properties of the alternating parity bands of Ra, Th, U and Pu isotopes assuming oscillations in the mass asymmetry degree of freedom is suggested. The existing experimental data on the angular momentum dependence of parity splitting and on multipole transition moments are quite well reproduced. The characteristics of the Hamiltonian used in the calculations were determined by investigating a completely different phenomenon, namely, heavy ion reactions at low energies.

T.M.S. and R.V.J. are grateful to BMBF and DFG (Bonn), respectively, for support. This work was supported in part by Volkswagen-Stiftung (Hannover), DFG (Bonn) and RFBR (Moscow). The support of STCU(Uzb-45), SCST and UFBR (Tashkent) is acknowledged as well.

REFERENCES

[1] W. Greiner, J.Y. Park, W. Scheid, *Nuclear Molecules*, World Scientific, Singapore 1995.

[2] W. Nazarewicz, J. Dobaczewski, *Phys. Rev. Lett.* **68**, 154 (1992).

[3] S. Cwiok *et al.*, *Phys. Lett.* **B322**, 304 (1994).

[4] S. Aberg, L.–O. Jonsson, *Z. Phys.* **A349**, 205 (1994).

[5] V.V. Pashkevich *et al.*, *Nucl. Phys.* **A624**, 140 (1997).

[6] M. Brack *et al.*, *Rev. Mod. Phys.* **44**, 320 (1972).

[7] G.G. Adamian, N.V.Antonenko, W. Scheid, *Nucl. Phys.* **A678**, 24 (2000).

[8] G.G. Adamian, N.V.Antonenko, W. Scheid, V.V. Volkov, *Nucl. Phys.* **A633**, 409 (1998).

[9] D.R. Inglis, *Phys. Rev.* **96**, 1059 (1954).

[10] F. Barranco, G.F. Bertsch, R.A. Broglia, E. Vigezzi, *Nucl. Phys.* **A512**, 253 (1990).

[11] A. Sobiczewski *et al.*, *Sov. J. Part. Nucl.* **10**, 466 (1979).

[12] A. Sobiczewski *et al.*, *Nucl. Phys.* **A131**, 67 (1969).

[13] G.G. Adamian, N.V. Antonenko, A.Diaz–Torres, W. Scheid, *Nucl. Phys.* **A671**, 233 (2000).

[14] G.G. Adamian, N.V. Antonenko, Yu.M. Tchuvilsky, *Phys. Lett.* **B451**, 289 (1999).

[15] A. Diaz-Torres *et al.*, *Phys. Lett.* **B481**, 228 (2000).

[16] X. Wu *et al.*, *Phys. Rev. Lett.* **79**, 4542 (1997).

[17] V.V. Pashkevich, *Nucl. Phys.* **A169**, 275 (1971).

[18] A. Sobiczewski *et al.*, *Nucl. Phys.* **A485**, 16 (1988); *Nucl. Phys.* **A473**, 77 (1987).

[19] A. Sobiczewski, K. Böning, *Acta Phys. Pol. B* **18**, 393 (1987).

[20] W.D.M. Rae, *Int. J. Mod. Phys.* **A3**, 1343 (1988).

[21] M. Freer, A.C. Merchant, *J. Phys. G* **23**, 261 (1997).

[22] V.V. Volkov, *Phys. Rep.* **44**, 93 (1978).

[23] S. Hofmann, G. Münzenberg, *Rev. Mod. Phys.* **72**, 733 (2000).

[24] Yu.Ts. Oganessian, *et al.*, *Nucl. Phys.* **A682**, 108c (2001).

[25] G.G. Adamian *et al.*, *Int. J. Mod. Phys.* **E5**, 191 (1996).

[26] G.G. Adamian *et al.*, *Phys. Part. Nucl.* **25**, 583 (1994).

[27] T.M. Shneidman, G.G. Adamian, N.V. Antonenko, R.V. Jolos, W. Scheid, *Phys. Lett.* **B526**, 322 (2002).

[28] J. Dudek, *Prog. Part. Nucl. Phys.* **28**, 131 (1992).

[29] T.M. Shneidman *et al.*, *Nucl. Phys.* **A671**, 119 (2000).

[30] P. Möller *et al.*, *At. Data and Nucl. Tables* **59**, 185 (1995).

[31] G.G. Adamian, N.V. Antonenko, R.V. Jolos, *Nucl. Phys.* **A584**, 205 (1995).

[32] http://www.nndc.bnl.gov/nndc/ensdf/

[33] Yu.S. Zamiatin *et al.*, *Phys. Part. Nucl.* **21**, 537 (1990).

[34] A. Bohr, B.R. Mottelson, *Nuclear Structure*, Vol. II, Benjamin, New York 1975.

[35] I. Hamamoto, *Nucl. Phys.* **A557**, 515c (1992).

[36] P.A. Butler, W. Nazarewicz, *Rev. Mod. Phys.* **68**, 350 (1996).

[37] J.F.C. Cocks *et al.*, *Nucl. Phys.* **A645**, 61 (1999).

[38] H.J. Wollersheim *et al.*, *Nucl. Phys.* **A556**, 261 (1993).

[39] S. Raman *et al.*, *At. Data Nucl. Data Tables* **36**, 1 (1987).